The Cryopreservation of Liposomes. 1. A Differential Scanning Calorimetry Study of the Thermal Behavior of a Liposome Dispersion Containing Mannitol During Freezing/Thawing

Herre Talsma,[1,3] Mies J. van Steenbergen,[1] Paul J. M. Salemink,[2] and Daan J. A. Crommelin[1]

Received June 11, 1990; accepted November 14, 1990

The thermal behavior of water in liposome dispersions and in liposome dispersions containing mannitol at subzero temperatures was investigated with differential scanning calorimetry (DSC). The cooling curves from 20 down to −60°C for a liposome dispersion (bilayer composition PL100H/DCP), monitored at cooling rates of 5 and 10°C/min, showed several heat flows related to water crystallization. All lipid-containing dispersions showed water crystallization at temperatures below −40°C. The magnitude of this heat flow strongly depended on the experimental variables. Cooling rate, particle size, lipid concentration, and location and nature of the cryoprotectant all influenced the water crystallization behavior as shown in the DSC cooling curve. Different fractions of water—presumably related to their location in the dispersion—could be distinguished. It is concluded that DSC provides a valuable tool for the detection of changes in the physical state of water in liposome dispersions during freezing/thawing. The insights gained from these DSC studies may make it possible to select—on the basis of rational considerations rather than by trial and error—optimum conditions for the cryopreservation of liposomes containing water-soluble drugs.

KEY WORDS: liposome; differential scanning calorimetry (DSC); stability; freezing/thawing; cryopreservation.

INTRODUCTION

Liposomes have been investigated for use as delivery systems for the controlled release of drugs, as carriers for site-specific delivery of drugs, and as antigen-presenting vehicles in vaccines (1–5). However, problems with the stability of liposome dispersions, especially dispersions of liposomes containing water-soluble, non-bilayer interacting drugs, may hamper or delay the introduction of liposomal products in therapy. Several ways to improve the shelf life of liposomes have been investigated, including proliposomes (6,7), storage of concentrated liposome dispersions (8), spray-drying of the liposome dispersions (9), and freezing or freeze-drying of the dispersions (10). For drugs interacting strongly with the bilayer, stable liposome dispersions can be prepared through freeze-drying or the preparation of proliposomes. Neither of the above-mentioned techniques has yet produced clinically acceptable liposomes for water-soluble, non-bilayer interacting drugs with an acceptable shelf life of several years. For this category of drugs, freeze-drying of the drug containing liposome dispersion is an attractive, but yet to be realized, option. Extensive drug release from the liposomes after the freeze-drying/rehydration cycle has been reported (10,11). The phenomena that occur during freeze-drying of a liposome dispersion are complex and poorly understood. The large number of variables in both the freeze-drying technique and the liposome dispersions (temperature and pressure program, residual moisture, lipid composition and concentration, particle size, cryoprotectants, and volumes used) makes it difficult to reduce leakage during freeze-drying. Therefore, in this study only the freezing step in the total freeze-drying process was considered. For practical reasons the full freezing/thawing cycle of liposome dispersions was taken into account. The objective was to investigate the crystallization behavior of water in liposome dispersions during freezing/thawing of these dispersions. Much of the potential damage to liposomes during freezing/thawing is directly related to the behavior of "water" in the dispersions: crystallization of internal water (i.e., water inside the vesicles), formation of amorphous material, dehydration of the lipid bilayers, and osmotic forces. Differential scanning calorimetry (DSC) was used to detect some of these different events. Calorimetry is a useful technique because water has a large crystallization enthalpy (12). Even small changes in the system because of water crystallization/melting can be detected.

MATERIALS AND METHODS

Phospholipon 100H (hydrogenated soybean phosphatidylcholine; PL100H) was a gift from Nattermann (Köln, FRG). Dicetylphosphate (DCP) was supplied by Sigma Chemicals (St. Louis, MO). Mannitol, glycerol, and propylene glycol met the requirements of the Ph. Eur. All chemicals were used as received. Negatively charged vesicles were prepared with the classical "film method" as described by Fransen *et al.* (13). All vesicle preparations had the same bilayer composition (PL100H/DCP at a molar ratio 10/1). Lipid phosphorous was determined according to the procedure of Fiske and Subbarow (14). Narrow vesicle size distributions were obtained by extruding the vesicles through polycarbonate filters with a defined pore size (Uni-pore, Bio-Rad, Richmond, CA). In all dispersions a buffer solution containing 10 m*M* Tris buffer (pH 7.4) was used. Mannitol was added at a concentration of 11.2% (m/m). A Netzsch DSC 200 low-temperature DSC was used (Netzsch-Gerätebau GMBH, Selb, FRG). This is a computer-controlled heat-flux DSC system which allows a programmable temperature control over a wide range of cooling/heating rates. Aliquots (8–25 μl) of the liposomal dispersion/solutions were put into aluminium pans. Introduction of 8 μl of the dispersions enabled the total heat flux to be monitored. Higher quantities caused a heat-flux overflow of the system at "bulk water" nucleation and melting. A small pin hole in the lid allowed for constant (atmospheric) pressure. As a reference an empty aluminium pan was used. Temperature scale and heat flux were calibrated with gallium and mercury.

[1] Department of Pharmaceutics, Faculty of Pharmacy, Utrecht University, P.O. Box 80.082, 3508 TB Utrecht, The Netherlands.
[2] Organon International BV., Oss, The Netherlands.
[3] To whom correspondence should be addressed.

0724-8741/91/0800-1021$06.50/0

Particle size was determined by dynamic light scattering with a Malvern 4700 system, using the automeasure vsn 3.2 software (Malvern Ltd., Malvern, GB). For all dispersions the value shown is the mean of three measurements. In the calculation of the particle size from the light-scattering data, the viscosity and refractive index of pure water were used, except for the dispersions containing mannitol outside the vesicles. Here the literature values of the viscosity and refractive index of the mannitol solution were utilized.

In order to estimate the amount of water involved in the different crystallization steps, it is necessary to correct the heat flux of water (dH as J/g) for temperature dependency (15). For the dH of water crystallization at temperatures below 0°C, the following equation is valid;

$$dH_i = dH_0 - \int_0^i (C_{pl} - C_{ps}) \cdot dT \qquad (1)$$

dH_0 is the crystallization enthalpy of water at 0°C (J/g), C_{pl} the heat capacity of water (J/g °C), and C_{ps} the heat capacity of ice (J/g °C). Assuming that the total heat transfer is due to water crystallization, the amount of water crystallizing in the different exothermic peaks can be estimated. From these data an estimation can be made of the amount of "noncrystallized" water [water not frozen in crystalline-state ice I (16)] in the dispersion. In the calculations a value of 2.1 J/g °C is used for $c_{pl} - c_{ps}$. For temperatures below −25°C this value may be too low according to measured heat capacities in water/heptane emulsions (16).

RESULTS

Cooling/Heating Curves of Liposome Dispersions Containing Mannitol

Figure 1 displays a typical example of a set of DSC cooling/heating curves for cooling/heating rates of 10°C/min. The heat flow vs temperature of the cooling scan (Fig. 1A) and heating scan (Fig. 1B) are shown. Six different solutions/liposome dispersions were investigated. (See Fig. 1 caption.)

The dispersions were cooled/heated at a rate of 10°C/min from 0 to −60°C, and vice versa. In Table I the mean extrapolated onset temperature ($T_{e.o.}$) and mean heat flow (dH) of the different peaks identified in Fig. 1 are shown.

In the cooling curve one to three exothermic heat flows were detected. In all curves a large heat flow associated with the crystallization of "bulk" water is shown (peak 1). For this "heterogeneous nucleation process" (16) the onset temperature lies around −15°C, indicating that some undercooling occurs before nucleation starts. Heterogeneous nucleation of water depends on the presence of crystallization nuclei. Therefore the crystallization onset temperature of the bulk water is not fixed on the temperature scale but is subject to fluctuations, as demonstrated by the relatively large standard deviation of the $T_{e.o.}$ of this peak. The curves of the lipid containing dispersions showed a second exothermic heat flow below −40°C (peak 2). The onset temperature of this crystallization process was fixed at a defined temperature as shown by the small standard deviation. Only for the dispersion containing mannitol both inside the vesicles and in the outside medium were large heat flows below −40°C found. For the dispersion containing mannitol inside the vesicles and Tris buffer in the outside medium (Fig. 1A, f), a third exothermic heat flow between the crystallization of the bulk water and the second exothermic heat flow below −40°C was found (peak 3). The onset temperature of this peak was also fixed at a defined temperature. In the heating curves (Fig. 1B) both the mannitol solution and the liposome

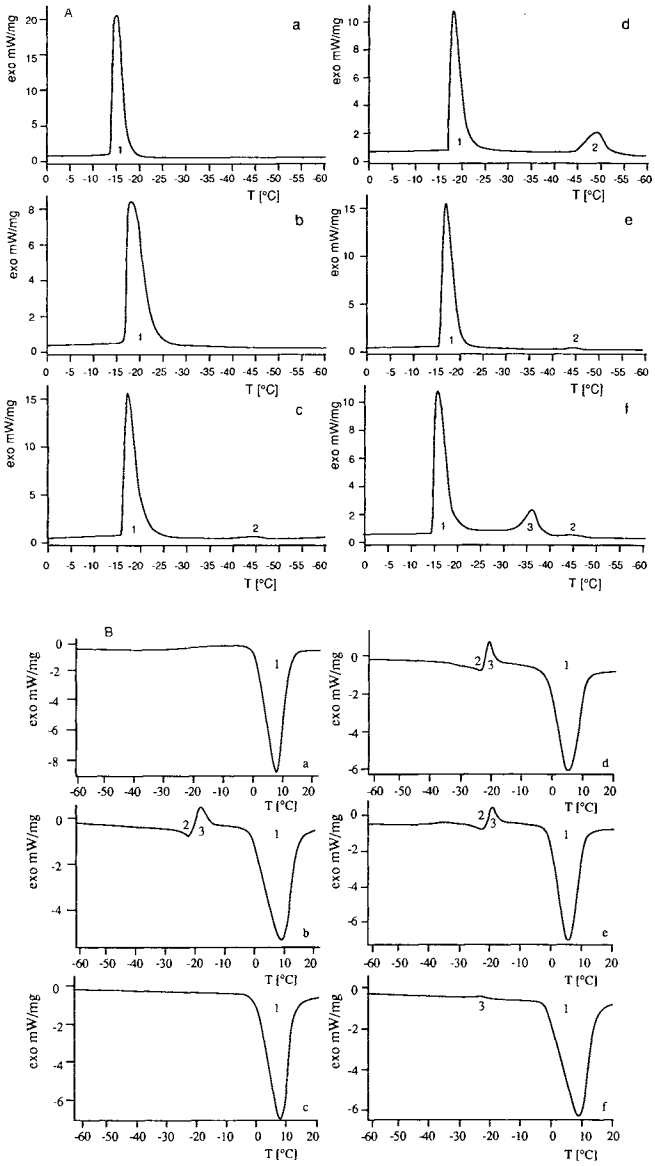

Fig. 1. Heat flux vs temperature. (A) Cooling curves; (B) heating curves. Cooling/heating rate, 10°C/min. A "typical example" is shown. (a) 10 mM Tris buffer, pH 7.4. (b) 11.2% mannitol in 10 mM Tris buffer, pH 7.4. (c) 32 μmol lipid/ml in 10 mM Tris buffer, pH 7.4; particle size, 0.32 μm; p.d., 0.4. (d) 35 μmol lipid/ml; 11.2% mannitol in 10 mM Tris buffer, pH 7.4, both inside the vesicles and in the outside medium; particle size, 0.32 μm; p.d., 0.4. (e) 33 μmol lipid/ml; 11.2% mannitol in 10 mM Tris buffer, pH 7.4, in the outside medium and 10 mM Tris buffer, pH 7.4, inside the vesicles; particle size, 0.27 μm; p.d., 0.4. (f) 35 μmol lipid/ml; 11.2% mannitol in 10 mM Tris buffer, pH 7.4, inside the vesicles; outside medium, 10 mM Tris buffer, pH 7.4; particle size, 0.32 μm; p.d., 0.4.

Table I. Extrapolated Onset Temperature ($T_{e.o.}$) and Heat Flows of the Different Peaks in Fig. 1[a]

No.	Peak 1		Peak 2		Peak 3	
	$T_{e.o.}$ (°C)	dH (J/g)	$T_{e.o.}$ (°C)	dH (J/g)	$T_{e.o.}$ (°C)	dH (J/g)
			(A) Cooling run			
a	−15.9 ± 1.2	293 ± 8				
b	−16.2 ± 1.5	225 ± 5				
c	−14.9 ± 1.1	258 ± 3	−41.9 ± 0.3	2.0 ± 0.4		
d	−14.5 ± 3.4	155 ± 2	−44.8 ± 0.1	43.8 ± 1.7		
e	−15.9 ± 2.0	242 ± 4	−42.7 ± 0.0	2.1 ± 0.1		
f	−14.2 ± 1.0	189 ± 4	−42.2 ± 0.3	2.7 ± 0.2	−32.8 ± 0.4	35.5 ± 1.8
			(B) Heating run			
a	−0.1 ± 0.4	−337 ± 5				
b	−1.7 ± 0.3	−285 ± 5	−29.9 ± 1.1	−12.7 ± 3.0	−20.6 ± 0.6	18.3 ± 2.2
c	−0.2 ± 0.2	−300 ± 2				
d	−2.1 ± 0.5	−270 ± 5	−33.6 ± 0.6	−15.8 ± 1.4	−22.6 ± 0.3	20.7 ± 1.1
e	−1.7 ± 0.6	−303 ± 8	−31.7 ± 0.7	−9.7 ± 1.8	−21.7 ± 0.4	15.9 ± 1.3
f	−2.3 ± 0.5	−321 ± 5			−26.2 ± 0.1	2.2 ± 0.6

[a] Cooling/heating rate, 10°C/min. For explanation of Nos. a–f, see the legend to Fig. 1. Mean ± standard deviation; n = 3.

dispersions containing mannitol in the outside medium showed a devitrification effect. First, a small endothermic heat flow was detected, followed by an exothermic effect. This exothermic heat flow is ascribed to crystallization of water in the solution/dispersion which did not crystallize during cooling but formed a glassy/amorphous mass. On rewarming of the system, part of this mass first thawed, allowing the rest of the water in the glassy/amorphous mass to crystallize as ice. The devitrification of the liposome dispersion containing mannitol occurred somewhat earlier on reheating than for the mannitol solution. A small freezing-point depression was found for the mannitol-containing solution/dispersions.

Factors Regulating the Crystallization Onset Temperature and Heat Flow of Peak 2

The onset temperature of the lipid-associated peak 2 (Fig. 1A) was dependent on the additives in the dispersion as shown in Table II. Here the additives were present both inside the vesicles and in the outside medium. The additives were selected for their cryoprotective potency (10). The concentrations were chosen arbitrary.

Table II. Extrapolated Crystallization Onset Temperature of the Lipid-Associated Peak for Different Cryoprotectants[a]

Cryoprotectant	% (m/m)	$T_{e.o.}$ (°C)
—	—	−41.9
Mannitol	11.2	−44.8
Glycerol/mannitol	10/10	−48.7
Glucose	30	−52.7
Glycerol	30	−61.3
Propylene glycol	30	−76.1

[a] $T_{e.o.}$: extrapolated onset temperature of the peak. Composition, Phospholipon 100H/dicetylphosphate (10/1); lipid concentration, 30–50 μmol/ml; buffer, 10 m*M* Tris buffer, pH 7.4; cooling rate, 10°C/min; particle size, about 0.3 μm.

In Table III the influence of particle size on the crystallization onset temperature and heat flow of peak 2 for a liposome dispersion in Tris buffer is shown. The smaller the particle size, the lower the extrapolated crystallization onset temperature of the lipid-associated peak in the dispersion. This reduction of the onset temperature is relatively small. The maximum heat flow for the liposome associated peak was found for a particle size of 0.2 μm.

In Fig. 2 the effect of reducing the cooling rate from 10 to 5°C/min on the mannitol solution (panel 1) and on the lipid-associated peak 2 for a dispersion in Tris buffer (panel 2) and in mannitol/Tris buffer (panel 3) is shown. For the mannitol solution a small heat flow at −35°C associated with crystallization of part of the mannitol-"associated" water was found. Further, the "bulk" water peak of the liposome dispersion in Tris buffer showed a shoulder. The liposome dispersion in mannitol/Tris buffer showed a double peak around −41°C.

For the heating curve no significant differences with the results obtained with a heating rate of 10°C/min were found (results not shown).

Heat Flow of the Liposome-Associated Peak After Isothermal Storage at −25°C

In Fig. 2 a double peak around −40°C was found for the liposome dispersion containing mannitol both inside the vesicles and in the external medium. To investigate the time dependency of the amount of heat released around −40°C, a special cooling program was used. The dispersions were directly placed in the precooled DSC chamber at −25°C, then stored isothermally at this temperature for different time periods and subsequently cooled down to −60°C with a cooling rate of 5°C/min. In these cooling curves three peaks were found: the bulk water crystallizing immediately after placing

Table III. Influence of the Particle Size on the Extrapolated Onset Temperature and Heat Flow of the "Bulk" Water and "Lipid-Associated" Peak[a]

Particle size (μm)	p.d.	Peak 1 $T_{e.o.}$ (°C)	Peak 1 dH (J/g)	Peak 2 $T_{e.o.}$ (°C)	Peak 2 dH (J/g)
0.87	0.6	−10.6 ± 2.3	269 ± 6	−39.8 ± 0.1	2.9 ± 0.3
0.33	0.4	−12.8 ± 1.8	266 ± 11	−40.3 ± 0.1	7.5 ± 0.2
0.25	0.2	−11.8 ± 2.5	269 ± 14	−40.7 ± 0.1	9.0 ± 1.3
0.20	0.1	−13.1 ± 2.2	263 ± 13	−41.2 ± 0.1	11.3 ± 0.2
0.14	0.1	−14.6 ± 1.4	268 ± 9	−41.4 ± 0.1	7.0 ± 0.4

[a] p.d., polydispersity; $T_{e.o.}$, extrapolated onset temperature of the peak. Composition, Phospholipon 100H/dicetylphosphate (10:1) in 10 m*M* Tris buffer, pH 7.4; lipid concentration, 30 μmol/ml; cooling rate, 10°C/min; $n = 3$.

the DSC pan in the chamber, a heat flow after approximately 3–5 min in the isothermal part, and a heat flow around −45°C in the cooling part. In Table IV the heat flow at −45°C in the cooling part, after different isothermal storage times, is shown.

This heat flow was time dependent. The longer the isothermal storage time at −25°C, the smaller the heat flow at −45°C.

The Relation Between Heat Flows at Temperatures Below −25°C and Lipid Concentration in the Presence of Mannitol

In Fig. 3 the relation between the heat flow of peaks 2 and 3 (Fig. 1A, d–f) and lipid concentration is shown for a cooling rate of 10°C/min. Large heat flows and a linear relation between lipid concentration and heat flow in peak 2 were found for the dispersion containing mannitol both inside the vesicles and in the external medium (Fig. 1A, d) and for peak 3 of the dispersion containing mannitol inside and Tris buffer in the external medium (Fig. 1A, f). Relatively small heat flows in peak 2 were found for the dispersion containing mannitol in the external medium and Tris buffer inside the vesicles (Fig. 1A, e) and for peak 2 of the dispersion containing mannitol inside and Tris buffer in the external medium (Fig. 1A, f). For the small heat flows a more or less linear relation between the amount of heat released and the lipid concentration in the dispersion was found.

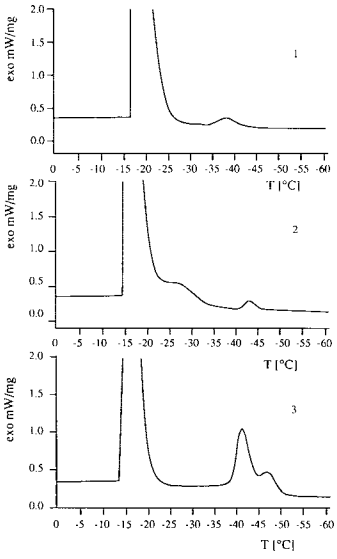

Fig. 2. Heat flux vs temperature. Cooling curves. Cooling rate, 5°C/min. (1) 11.2% (m/m) mannitol in 10 m*M* Tris buffer, pH 7.4. (2) 50 μmol lipid/ml; in 10 m*M* Tris buffer, pH 7.4. (3) 50 μmol lipid/ml; 11.2% (m/m) mannitol in 10 m*M* Tris buffer, pH 7.4, both inside the vesicles and in the outside medium; particle size, about 0.3 μm.

Crystallization Behavior with Mannitol Present Only in the External Medium

In Fig. 4 the influence of the lipid concentration is shown on the crystallization behavior of the dispersion containing mannitol outside and Tris buffer inside the vesicles at a cooling rate of 5°C/min. As reference the behavior of mannitol in Tris buffer is shown (Fig. 4, 1). Dispersions with high lipid concentrations (Fig. 4, 2) behaved in the same way as was found for these dispersions at a cooling rate of 10°C/min (Fig. 1A, d). However, dispersions with low lipid concentrations (Fig. 4, 4) behaved like pure mannitol/Tris buffer solutions without lipid at this cooling rate (cf. Fig. 2, 1).

DISCUSSION

This study was performed to shed light on the behavior of water–lipid dispersions at subzero temperatures to help in the rational design of stable liposomes by means of freeze-drying. Mannitol was added to the dispersions, as it is commonly used as a "cake-forming" agent in pharmaceutical preparations. Although it is an excellent cake-forming agent, the cryoprotective activity is reportedly poor (10,13). For the freezing behavior of water and aqueous solutions (16),

Table IV. Crystallization Heat of the Liposome-Associated Peak (Around −45°C) After Different Isothermal Storage Times at −25°C

Isothermal time (min)	Crystallization heat (J/g)
4	5.0
9	2.4
18	1.5

[a] Composition, Phospholipon 100H/dicetylphosphate (10:1); concentration, 50 μmol/ml lipid in 11.2% mannitol, 10 m*M* Tris buffer, pH 7.4; particle size, ±0.3 μm.

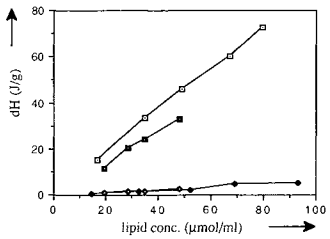

Fig. 3. Heat flow (J/g) vs lipid concentration (μmol/ml) of peaks 2 and 3 in Fig. 1A, panels d, e, and f. Cooling rate, 10°C/min. Particle size, ±0.3 μm. (—□—) Peak 2, Fig. 1A, panel d (Tris buffer/mannitol both inside the vesicles and in the outside medium). (—♦—) Peak 2, Fig. 1A, panel e (Tris buffer inside the vesicles, Tris buffer/mannitol in the outside medium). (—■—) Peak 3, Fig. 1A, panel f (Tris buffer/mannitol inside the vesicles, Tris buffer in the outside medium). (—◇—) Peak 2, Fig. 1A, panel f (Tris buffer/mannitol inside the vesicles, Tris buffer in the outside medium).

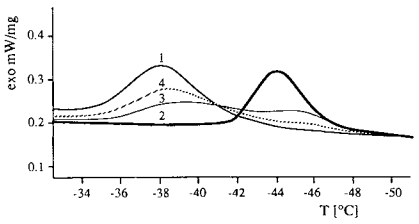

Fig. 4. Heat flow vs temperature of a Tris buffer/mannitol solution and three dispersions containing different amounts of lipid in Tris buffer/mannitol. Cooling rate, 5°C/min. (1) 11.2% mannitol in 10 m*M* Tris buffer, pH 7.4. (2) 93 μmol lipid/ml; inside the vesicles 10 m*M* Tris buffer, pH 7.4; outside medium, 11.2% mannitol in 10 m*M* Tris buffer, pH 7.4. (3) 33 μmol lipid/ml; inside the vesicles 10 m*M* Tris buffer, pH 7.4; outside medium, 11.2% mannitol in 10 m*M* Tris buffer, pH 7.4. (4) 15 μmol lipid/ml; inside the vesicles 10 m*M* Tris buffer, pH 7.4; outside medium, 11.2% mannitol in 10 m*M* Tris buffer, pH 7.4.

two different nucleation conditions yielding crystalline ice can be distinguished: heterogeneous nucleation, where crystallization is started by impurities, and homogeneous nucleation, where the water molecules/aqueous solutions undergo spontaneous crystallization in the absence of any impurity. Crystallization and melting are detected by an exothermic and endothermic peak, respectively, in the DSC curves. Apart from crystalline ice, amorphous/glassy material (only a small shift in the baseline) can be formed during cooling. The formation of amorphous mass is dependent on the presence of cryoprotectant or other additives and cooling conditions. Upon rewarming devitrification of amorphous material may be observed in the DSC curves (a small endothermic heat flow followed by a much larger exothermic heat flow; Fig. 1B, peak 2/3). The heat flow of peak 2 in Fig. 1A is associated with the homogeneous nucleation of water. The extrapolated onset temperatures of peak 2 for different cryoprotectant containing solutions as shown in Table II are in good agreement with the homogeneous nucleation temperatures published by MacKenzie (17), (measured with differential thermal analysis) for the Rasmussen/MacKenzie water–cryoprotectant/heptane emulsions.

For all lipid-containing dispersions in Fig. 1 a heat flow at the homogeneous nucleation temperature indicates that part of the water in the dispersions is protected against crystallization by the presence of phospholipid until the homogeneous nucleation temperature is reached. It is suggested that (part of) the internal volume of the vesicles is protected against heterogeneous nucleation, by the limited volume of encapsulated water inside the liposome and/or the presence of additives. The smaller the particle size, the more probable is solidification of the internal volume to occur at the homogeneous nucleation temperature. The presence of mannitol both in- and outside the vesicles tends to prohibit internal crystallization before the homogeneous nucleation temperature is reached, in particular, for those vesicles with a small size (Table III). The larger particles have a chance to nucleate before the homogeneous nucleation temperature is reached, because of their larger internal volume.

For the mannitol solution crystallization of mannitol itself in the solution might contribute to the total heat flow. Calculation of the total heat transfer during cooling/rewarming (Table I) shows that the total amount of heat transferred is not significantly different from that during cooling/rewarming of the Tris buffer if the heat flow is corrected for the lower amount of water present in the mannitol dispersion. Therefore, all the effects shown in the DSC curves are related to the behavior of "water" in the dispersions. However, mannitol influences the crystallization behavior of water. This is clearly demonstrated if the cooling rate is changed. If a cooling rate of 10°C/min is used, no mannitol-associated heat flow is found in the DSC cooling curves (Fig. 1A) and a clear devitrification effect is present in the heating curves (Fig. 1B, peak 2/3). A cooling rate of 5°C/min shows a mannitol-associated crystallization effect in the cooling curves (Fig. 4, peak 1) and a smaller devitrification effect in the heating curves (not shown). Cooling rates of 10°C/min and higher cause the formation of amorphous material because of the presence of mannitol in the freezing cake, while cooling rates of 5°C/min and less allow (part of) the mannitol to crystallize during cooling as shown by the small exothermic heat flow caused by the crystallization of water set free as soon as mannitol crystallizes.

Several variables influence the amount of heat released at the homogeneous nucleation temperature: cooling rate, particle size (Table III), presence and location of mannitol (Fig. 1, Table I), lipid concentration (Fig. 4), and storage time below 0°C (Table IV). The physical state of a vesicle dispersion after "freezing" is dependent on the combination of these parameters. The data in Table IV show that even after 18 min of storage at −25°C, part of the dispersion still crystallizes at the homogeneous nucleation temperature. For the cryoprotectants (Table II) the homogeneous nucleation temperature is even lower than for mannitol solutions. This strongly suggests that part of the reportedly "frozen" dispersions were only partly frozen during freeze-drying and, in addition to a crystalline/amorphous/glassy mass, still contained "freezable" water (11). This condition could explain some of the earlier partially successful short-term freezing/thawing experiments with water-soluble markers inside the liposomes (11) and the lack of success when these dispersions were freeze-dried. Part of the water in the dispersion was not completely converted into ice before freeze-drying. It emphasizes the necessity for a clear description of

the samples under investigation and the freezing protocol for the dispersions.

The importance of the localization of mannitol in the dispersion on the magnitude of peaks 2 and 3 (Fig. 1A) is demonstrated in Fig. 3. The presence of mannitol both inside the vesicles and in the outside medium seems necessary to protect against crystallization before the homogeneous nucleation temperature is reached. Assuming that the total heat flow of the mannitol-containing dispersions at the homogeneous nucleation temperature is due to crystallization of the encapsulated water (Fig. 1A, d), the encapsulated volume can be calculated. An encapsulated volume of 5.4 ± 0.2 L/mol lipid for a particle size of 0.32 μm is found. If peak 3 in Fig. 1A, f (only mannitol inside), is used to calculate the encapsulated water, 3.9 ± 0.1 L/mol lipid is found for the same particle size. These values are somewhat lower than the 6.5 ± 0.5 L/mol lipid that was calculated for a similar dispersion, when the encapsulated volume was determined with the carboxyfluorescein method (18). Part of the discrepancy between the data from both methods may be due to an underestimating of the amount of freezing water, the c_p of water below −38°C is not exactly known but increases sharply (15). Moreover, part of the internal volume might not crystallize but form a glassy/amorphous mass or part of the vesicles (the larger vesicles?) may already crystallize before the homogeneous nucleation temperature is reached.

The results show a complex freezing/thawing behavior of the liposome dispersions. Cooling rate, particle size, lipid concentration, and localization and nature of the additives all affect the crystallization behavior of water in the dispersions. With DSC it is possible to establish the crystallization behavior of different water fractions in the dispersions under various conditions. This provides a valuable tool for the detection of changes in the physical conditions of the dispersions during freezing/thawing. At the present, however, it is still unclear under what freezing/thawing conditions leakage of non-bilayer interacting encapsulated molecules can be prevented.

NOMENCLATURE

c_{pl}	Heat capacity of the liquid phase, J/g °C
c_{ps}	Heat capacity of the solid phase, J/g °C
DCP	Dicetylphosphate
DSC	Differential scanning calorimetry
dH_0	Crystallization enthalpy at 0°C, J/g
dH	Heat flow, J/g
PL100H	Hydrogenated soy-bean phosphatidylcholine
p.d.	Polydispersity, index for width of particle size distribution: 0 = monodisperse
$T_{e.o.}$	Extrapolated onset temperature

REFERENCES

1. G. Gregoriadis (ed). *Liposome Technology. Volume III. Targeted Drug Delivery and Biological Interaction,* CRC Press, Boca Raton, FL, 1984.
2. M. J. Ostro. *Liposomes: From Biophysics to Therapeutics,* Marcel Dekker, New York, 1987.
3. R. L. Juliano and D. Layton. Liposomes as a drug delivery system. In R. L. Juliano (ed.), *Drug Delivery Systems,* Oxford University Press, 1980, pp. 189–236.
4. F. H. Roerdink, T. Daemen, I. A. J. M. Bakker-Woudenberg, G. Storm, D. J. A. Crommelin, and G. L. Scherphof. Therapeutic utility of liposomes. In J. G. Lloyd-Jones and P. Johnson (eds.), *Drug Delivery Systems, Vol. 1,* Ellis Horwood, Chichester (GB), 1987, pp. 66–80.
5. G. F. A. Kersten, E. C. Beuvery, and D. J. A. Crommelin. Antigen presentation and adjuvants. In D. D. Breimer, D. J. A. Crommelin, and K. K. Midha (eds.), *Topics in Pharmaceutical Sciences 1989,* Amsterdam Medical Press/SDU, Noordwijk/The Hague (NL), 1989, pp. 313–322.
6. N. I. Payne, P. Timmins, C. V. Ambrose, M. D. Ward, and F. Ridgway. Proliposomes: A novel solution to an old problem. *J. Pharm. Sci.* 75:325–329 (1986).
7. N. I. Payne, I. Browning, and C. A. Hynes. Characterization of proliposomes. *J. Pharm. Sci.* 75:330–333 (1986).
8. H. Talsma, T. Klaver, E. v. Tuin, and D. J. A. Crommelin. Study of the stability of water-soluble drug containing liposomal dispersions after removing excess water by means of vacuum drying. *Acta Pharm Tech.* 34:22S (1988).
9. H. Hauser and G. Strauss. Stabilization of small unilamellar phospholipid vesicles during spray-drying. *Biochim. Biophys. Acta* 897:331–334 (1987).
10. Y. Özer, H. Talsma, D. J. A. Crommelin, and A. A. Hincal. Influence of freezing and freeze-drying on the stability of liposomes dispersed in aqueous media. *Acta Pharm. Tech.* 34:129–139 (1988).
11. D. J. A. Crommelin and E. M. G. van Bommel. Stability of liposomes on storage: Freeze dried, frozen or as an aqueous dispersion. *Pharm. Res.* 1:159–163 (1984).
12. R. C. Weast (ed.). Key values for thermodynamics. In *CRC Handbook of Chemistry and Physics,* 68th ed., CRC Press, Boca Raton, FL, 1978, pp. D–98.
13. G. J. Fransen, P. J. M. Salemink, and D. J. A. Crommelin. Critical parameters in freezing of liposomes. *Int. J. Pharm.* 33:27–35 (1986).
14. C. H. Fiske and Y. Subbarow. The colorimetric determination of phosphorus. *J. Biol. Chem.* 66:375–400 (1925).
15. C. A. Angell, M. Oguni, and W. J. Sichina. Heat capacity of water at extremes of supercooling and superheating. *J. Phys. Chem.* 86:998–1002 (1982).
16. C. A. Angell. Supercooled water. In F. Franks (ed.), *Water, a Comprehensive Treatise, Vol. 7. Water and Aqueous Solutions at Subzero Temperatures,* Plenum Press, New York, 1982, pp. 1–81.
17. A. P. MacKenzie. Non-equilibrium freezing behaviour of aqueous systems. *Phil. Trans. R. Soc. Lond. B* 278:167–189 (1977).
18. P. I. Lelkes. Methodological aspects dealing with stability measurements of liposomes in vitro using the carboxyfluorescein-assay. In G. Gregoriadis (ed.), *Liposome Technology, Vol. III. Targeted Drug Delivery and Biological Interaction,* CRC Press, Boca Raton, FL, 1984, pp. 225–246.